Multivariable Robust Controller for Linear and Angular Velocities of Electrically-Powered Wheelchair Using Characteristic Loci Method

Mohammad Nasser Saadatzi and Javad Poshtan

Abstract—A MIMO description of an Electrically-Powered Wheelchair (EPW) is developed using kinematics of non-holonomic mobile robots in addition to DC electric motors dynamics. The dynamics is augmented with an innovative static matrix in order to achieve diagonal dominance and to obtain a reliable estimation of the plant. Characteristic loci method is exploited to design a MIMO controller for the augmented system to fulfill ride comfort, safety as well as acceptable maneuverability. A sufficient stability theorem is checked to ensure robust stability for whole uncertainty range. Experimental results obtained from microcontroller-based implementation of the controller verify robust stability and desired performance of the control system.

I. INTRODUCTION

EPW Applications are growing as a consequence of increment in elderly people population and accidents [1]. Differential mechanism using 2 propelling wheels and 2 casters in EPWs has been the basic model of the majority of researches since 80's. In [2] and [3] a simple model of a DC electric motor was utilized for wheel speed control based upon PID technique. A robust optimal controller for the EPW based upon linear quadratic optimization was proposed in [4] which ensured asymptotic tracking and disturbance rejection. During 2000 to 2006, due to tendency to smart wheelchairs and path following problems, except neural networks-based speed control of the EPW wheel [5, 6], there were no outstanding activities. EPW was always observed as two electric motors with their speeds to track a desired profile. Until in [7], a dynamics of EPW was developed using its similarity to servomechanisms. The multivariable dynamics, afterwards, was reduced to two SISO dynamics, each controlled with a separate SISO controller using neural networks techniques.

In this paper, the dynamic equations of right and left electric motors in EPW and kinematic equations of non-holonomic mobile robots are combined together in order to develop a precise description of EPW dynamics which appears as a 2-input-2-output transfer-function matrix (TFM). The MIMO description of EPW dynamics benefits the controller design in an important way, in that the dynamics interaction among the EPW outputs, i.e. linear and angular velocities can be more obviously observed and systematically tackled. In the

next stage, CLM is exploited to design a controller satisfying time response requirements in addition to ride comfort and safety. In order to experimentally verify the proposed algorithm, an EPW has been constructed as shown in Fig. 1. Experimental results obtained from microcontroller-based implementation of the controller show the system performance.

Fig. 1. Typical EPW built in our laboratory.

II. DYNAMIC MODELING

In (1) and (2), the dynamic equations of right and left electric motors are presented [8]. Model parameters of the EPW are shown in Table I.

TABLE I
MODEL PARAMETERS

Symbol	Quantity
ω_l, ω_r	Left and right wheel angular velocities
K_{tl}, K_{tr}	Left and right motor torque constants
K_{el}, K_{er}	Left and right motor EMF constants
L_{al}, L_{ar}	Left and right motor wiring inductances
R_{al}, R_{ar}	Left and right motor wiring resistances
J_l, J_r	Left and right motor inertial moments
B_l, B_r	Left and right motor frictions
e_l, e_r	Left and right motor input voltages
R_l, R_r	Left and right wheel radii
W	Wheelchair width

$$\omega_l(s) = \frac{K_{tl}}{(L_{al}s+R_{al})(J_ls+B_l)+K_{tl}K_{el}} e_l(s) \quad (1)$$

$$\omega_r(s) = \frac{K_{tr}}{(L_{ar}s+R_{ar})(J_rs+B_r)+K_{tr}K_{er}} e_r(s) \quad (2)$$

A simplified mechanism of the EPW is illustrated in Fig. 2. P_0 is rear axle middle point with (x_0, y_0) coordinates. In this mechanism three constraints can be formulated.

Mohammad Nasser Saadatzi is with the Iran University of Science and Technology, Tehran, Iran (phone: 98-21-22503028; fax: 98-21-22313672; e-mail: mn_saadatzi@elec.iust.ac.ir).

Javad Poshtan is with the Iran University of Science and Technology, Tehran, Iran.
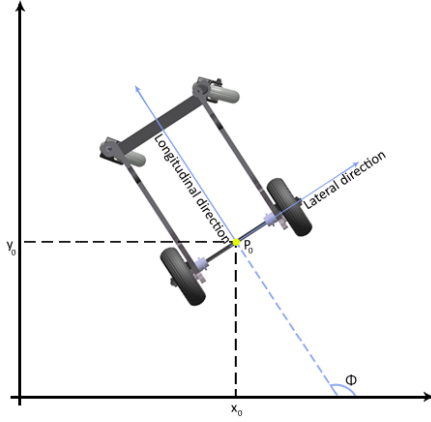
Fig. 2. EPW chassis. Seat and other parts are removed for better illustration of propelling system.

The first constraint states that EPW has no movement in the lateral direction, i.e.

$$\dot{y}_0 \cos\varphi - \dot{x}_0 \sin\varphi = 0 \tag{3}$$

Assuming no slippage rolling of rear wheels, the other two constraints appear as the following:

$$\dot{x}_0 \cos\varphi + \dot{y}_0 \sin\varphi + \frac{W}{2}\dot{\varphi} = R_r \omega_r \tag{4}$$

$$\dot{x}_0 \cos\varphi + \dot{y}_0 \sin\varphi - \frac{W}{2}\dot{\varphi} = R_l \omega_l \tag{5}$$

Subtracting (4) from (5) and integrating it with well-defined initial conditions yield angular velocity of point P_0 which, in the rest of this paper, is considered as EPW Angular Velocity and is represented by Ω.

$$\Omega = \frac{R_r}{W}\omega_r - \frac{R_l}{W}\omega_l \tag{6}$$

EPW Linear Velocity represented by V is considered as linear velocity of point P0. Geometric relations between EPW coordinate frame and the reference coordinate frame are formulated as follows:

$$V = \dot{x}_0 \cos\varphi + \dot{y}_0 \sin\varphi \tag{7}$$
$$\dot{x}_0 = V\cos\varphi \tag{8}$$
$$\dot{y}_0 = V\sin\varphi \tag{9}$$

Combination of (3), (4), (5), (7), (8) and (9) yields:

$$V = \frac{R_r}{2}\omega_r + \frac{R_l}{2}\omega_l \tag{10}$$

For more information refer to [9].

The EPW multivariable dynamic equation which appears as a 2-input-2-output TFM is released by mixing (1), (2), (6) and (10), as the following:

$$\begin{bmatrix} V(s) \\ \Omega(s) \end{bmatrix} = \begin{bmatrix} g_{11} & g_{12} \\ g_{21} & g_{22} \end{bmatrix}\begin{bmatrix} e_l(s) \\ e_r(s) \end{bmatrix} = G(s)E(s) \tag{11}$$

$$g_{11} = \frac{R_l K_{tl}/2}{(L_{al}s + R_{al})(J_l s + B_l) + K_{tl}K_{el}} \tag{12}$$

$$g_{12} = \frac{R_r K_{tr}/2}{(L_{ar}s + R_{ar})(J_r s + B_r) + K_{tr}K_{er}} \tag{13}$$

$$g_{21} = \frac{-R_l K_{tl}/W}{(L_{al}s + R_{al})(J_l s + B_l) + K_{tl}K_{el}} \tag{14}$$

$$g_{22} = \frac{R_r K_{tr}/W}{(L_{ar}s + R_{ar})(J_r s + B_r) + K_{tr}K_{er}} \tag{15}$$

III. ACQUIRING DIAGONAL DOMINANCE AND SYSTEM IDENTIFICATION

It is normally the time to identify the plant with the structures in (11) to (15). Identification of this TFM can be accomplished in two consecutive steps. First step includes stimulating e_l while keeping e_r to zero, measuring the outputs and estimating g_{11} along with g_{21}. In the second step, similarly, g_{12} and g_{22} are estimated the same way by solely stimulating e_r and recording the outputs. Identification through this approach, however, shows noticeable discrepancy between empirical and theoretical stimulation of the system. The reason of this fact is that merely stimulating e_l (e_r) results in a circular movement whose center is the ground contact point of the right (left) wheel and whose radius is the EPW rear wheelbase. Normal movement of EPW, however, is around longitudinal direction. Identification in this way suffers from another drawback, in that, it loses information about the motors interaction and their mutual effects since one of the motors is always off. To solve this problem, simultaneous stimulation of e_l and e_r is necessary which forces us to identify four SISO transfer functions simultaneously and involves multivariable identification methods. Moreover, appropriate application of CLM in the next stage needs TFM to be rather diagonal dominant (DD) while this matrix is not so at all:

$$g_{11} \cong g_{12} \ , \ \ g_{21} \cong -g_{22} \tag{16}$$

It is noteworthy that these small differences in (16) are consequences of lack of complete symmetry between corresponding physical parameters in either side of EPW. This matter is originated from asymmetry in electrical features of right and left motors in addition to their loads and frictions. The asymmetry in mechanical features like load and friction is due to occupant's manner of sitting which is time varying and not symmetric.

To circumvent all mentioned problems an innovative activity is devised in which G is decomposed as follows:

$$G = \beta\Gamma(s) \tag{17}$$

$$\beta = \begin{bmatrix} 1/2 & 1/2 \\ -1/W & 1/W \end{bmatrix} \tag{18}$$

$$\Gamma(s) = \begin{bmatrix} \frac{R_l K_{tl}}{(L_{al}s + R_{al})(J_l s + B_l) + K_{tl}K_{el}} & 0 \\ 0 & \frac{R_r K_{tr}}{(L_{ar}s + R_{ar})(J_r s + B_r) + K_{tr}K_{er}} \end{bmatrix} \tag{19}$$

In (17) Γ is diagonal unlike β. So the reason of the interaction is β. In (19) diagonal elements are nearly equal, so Γ can temporarily be assumed as:

$$\Gamma(s) \simeq \frac{R_l K_{tl}}{(L_{al}s+R_{al})(J_l s+B_l)+K_{tl}K_{el}}\begin{bmatrix} 1 & 0 \\ 0 & 1 \end{bmatrix} = \gamma(s).I_{2*2} \tag{20}$$

$$G(s) \simeq \gamma(s).\beta \tag{21}$$

Equation (20) implies that inverse of β can be utilized to reduce the interaction and achieve diagonal dominance (DD).

$$H \triangleq \beta\Gamma(s)\beta^{-1} = G\beta^{-1} \tag{22}$$

This pre-compensator considerably decouples the system. The more accurate (20) is, the higher DD of H is obtained.

$$\begin{bmatrix} V(s) \\ \Omega(s) \end{bmatrix} = G(s)E(s) = G(s)\beta^{-1}\beta E(s) = H(s)\beta E(s) \tag{23}$$

$$U(s) = \begin{bmatrix} u_1 \\ u_2 \end{bmatrix} \triangleq \beta E(s) = \begin{bmatrix} \frac{e_l+e_r}{2} \\ \frac{e_l-e_r}{W} \end{bmatrix} \tag{24}$$

$$H(s) = \begin{bmatrix} h_{11} & h_{12} \\ h_{21} & h_{22} \end{bmatrix} \tag{25}$$

Each element of matrix H is a transfer-function with two zeros and four poles with a format like the following:

$$h_{ij} = \frac{c_{ij}s^2+b_{ij}s+a_{ij}}{s^4+D_{ij}s^3+C_{ij}s^2+B_{ij}s+A_{ij}}, i,j = 1,2 \tag{26}$$

In the rest of the paper, the augmented system, H, is considered as the system to be dealt with and controlled. The new inputs, therefore, are u_1 and u_2. An advantage of this assumption is that H is much more DD compared to G and is more proper to be controlled using CLM in the next stage. Note the elements of H definitions according to (22):

$$h_{11} = g_{11} + g_{12} \tag{27}$$
$$h_{12} = \frac{W}{2}(-g_{11} + g_{12}) \tag{28}$$
$$h_{21} = g_{21} + g_{22} \tag{29}$$
$$h_{22} = \frac{W}{2}(-g_{21} + g_{22}) \tag{30}$$

Having (16) in mind, (27) to (30) reveal DD degree of H. It should be noticed that the new inputs are actually meaningful physical signals not just some definitions. Regarding (24) u_1 is the common component and u_2 is (proportional to) the difference component of two electric motors input voltages. Note that regarding (24), sole stimulation of either u_1 or u_2 causes both motors to operate simultaneously and hence, their interaction can be observed.

Another important advantage of dealing with H instead of G is that solely stimulating u_1 affects Ω insignificantly which makes EPW move about longitudinal direction. Hence, identification of h_{11} and h_{21} is more reliable. After identification of h_{11} and h_{21} only h_{12} and h_{22} remain to be estimated. Mere stimulation of u_2, however, affects Ω considerably. To prevent this, u_1 is stimulated constantly and u_2 is stimulated with a small-magnitude pseudo-random binary signal (PRBS) which results in a little crinkled movement around longitudinal direction. Theoretically, stimulating H with the same inputs identifies h_{12} and h_{22} since h_{11} and h_{21} are already known. Comparing the results of identical stimulation of EPW and H shows a high degree of correspondence. The estimated elements of H for the nominal system are:

$$h_{11} = \frac{18.9s^2+1260s+1.75}{s^4+274s^3+12485s^2+180384s+34.8} \tag{31}$$
$$h_{12} = \frac{0.4445s^2+23.44s+1.523}{s^4+677s^3+54613s^2+113943s+40800} \tag{32}$$
$$h_{21} = \frac{32s^2+3250s+4902}{s^4+29607s^3+3416644s^2+15604540s+3620877} \tag{33}$$
$$h_{22} = \frac{3.6s^2+3611s+5522}{s^4+981s^3+66127s^2+171689s+78214} \tag{34}$$

The most effective sources of uncertainty in our modeling are unspecified occupant weight and uncertain time varying center of gravity (COG) in addition to casters behavior. These uncertainties impose different propelling and frictional forces to each motor permanently or temporarily. Hence, EPW is run 100 times, and 100 TFMs are estimated. For each element of H, therefore, an additive uncertainty can be calculated. Let H_o denote true TFM of the augmented plant, then

$$H_o(s) = H(s) + \Delta(s) \tag{35}$$

where Δ represents an additive frequency-dependant perturbation whose upper bound is restricted as follows:

$$\Delta_{11} = h_{11}(0)\frac{0.72s+0.8}{1.1s+1} \tag{36}$$
$$\Delta_{12} = h_{12}(0)\frac{0.7s+1}{1.2s+1} \tag{37}$$
$$\Delta_{21} = h_{21}(0)\frac{0.7s+1}{1.2s+1} \tag{38}$$
$$\Delta_{22} = h_{22}(0)\frac{0.72s+0.8}{1.2s+1} \tag{39}$$

If the occupant weighs less and/or if COG approaches toward rear wheels, TFM magnitude increases and vice versa. If COG approaches towards the right or left side of EPW, DD of H decreases, in that, only off-diagonal elements of H increase without a significant variation in diagonal elements.

IV. CONTROL SYSTEM PERFORMANCE SPECIFICATIONS

Some criteria for the closed-loop system are established in order to fulfill ride comfort, maneuverability and safety:
1) Under-damped responses result in undesired vibrations which affect ride comfort. Maximum overshoot, hence, is defined as $M_p<5\%$.
2) Achieving acceptable maneuverability requires us to speed up the responses as much as it has no influence on ride comfort so $T_s<3$sec seems to be appropriate.

3) Wheelchair angular velocity varies if the system is subjected to a linear velocity disturbance or the occupant decides to speed up or slow down, and meanwhile there exists interaction between linear and angular velocities. Angular velocity variation turns into steering direction variation which may cause hitting to obstacles. So in order to strengthen safety, interaction must be definitely removed.

4) Since we are facing an uncertain model, it is necessary to obtain robust stability and desired performance in the whole uncertainty range.

V. CONTROL STRATEGY

In CLM, the controller design is accomplished in three stages described briefly below:

1) Design a static pre-compensator in order to debilitate interaction in high frequency band which, in fact, is a real approximation of TMF in a specified high frequency. This causes the whole system around that frequency to approach unity and removes interaction.

2) Design a dynamic pre-compensator in medium-frequency to improve transient behavior as well as stability margins.

3) Design a dynamic pre-compensator having integral nature to attain zero steady-state error and zero steady-state interaction.

In all stages, design should be done with the least influence on its previous stage. For more information refer to [10].

A. High-Frequency Compensation

Since according to parametric equations a high degree of DD was obtained in the previous section, this stage cannot achieve better DD. Therefore, this stage is skipped.

B. Medium-Frequency Compensation

An approximate commutative controller is designed in frequency 1 rads^{-1}. Real approximation of left eigenvector in this frequency, W_m, is calculated using ALIGN algorithm explained in [10]. A diagonal matrix with phase-lead elements, Λ_m, is designed to shape characteristic loci of H near cross-over frequency to achieve required transient features as well as maximum feasible stability margins.

$$W_m = \begin{bmatrix} 1 & 0.008 \\ -0.012 & 1 \end{bmatrix} \tag{40}$$

$$\Lambda_m(s) = \begin{bmatrix} \dfrac{23.89s+20}{0.84s+1} & 0 \\ 0 & \dfrac{32.68s+20}{0.61s+1} \end{bmatrix} \tag{41}$$

Final medium-frequency compensator is calculated as:

$$K_m(s) = W_m\Lambda_m(s)W_m^{-1} \tag{42}$$

C. Low-Frequency Compensation

This stage of CLM aims to remove steady-state error and steady-state interaction. Elements of the designed diagonal matrix are identical PI compensators.

$$K_l(s) = \left(\frac{0.27s+1}{2s}\right) * I_{2x2} \tag{43}$$

The complete compensator is acquired by multiplication of medium and low-frequency compensators as follows:

$$K(s) = K_m(s)K_l(s) = W_m\Lambda_m(s)W_m^{-1}K_l(s) \tag{44}$$

Closed loop stability is analyzed for all other 99 TFM's along with this controller using generalized Nyquist theorem. In case of instability for any TFM, the whole design level in section V must be repeated. The designed controller in (44) is actually obtained via a few iterations to fulfill stability for the whole uncertainty range. To ensure stability robustness, the following theorem is exploited.

Sufficient stability theorem for unstructured additive perturbation: Consider the additive model of uncertainty defined by (35). If $\Delta(s)$ is stable, that is, the plant unstable poles remain fixed as it varies over its uncertainty region then a sufficient condition to guarantee that instability cannot occur for any possible perturbation is:

$$\overline{\sigma}\left(\left(I + K(s)H(s)\right)^{-1}K(s)\Delta(s)\right) < 1 \tag{45}$$

Proof: refer to [10]. It can be seen in Fig. 3 that (45) holds for our system, indeed.
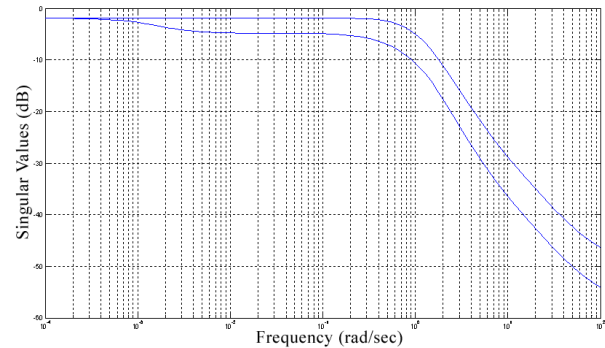

Fig. 3. Singular values of ((I+KH)$^{-1}$KΔ) which do not exceed 0 dB in all frequencies.

VI. IMPLEMENTATION AND RESULTS

The designed controller is accomplished as a series connection of 5 matrices, 1 matrix for achieving DD and 4 matrices for shaping characteristic loci by adding phase-lead and PI actions. The controller complexity is reasonable though as it can be minimally realized with 4 state variables. To discretize the controller a step time of 20 ms is considered which is very small compared to the time constant of the plant. As shown in Fig. 4 this controller is implemented in an Intel 8051 microcontroller. In control unit two ADC07's are responsible for reading the joystick potentiometers, and two DAC07's are in charge of commanding two voltage-controlled oscillators placed inside

the motors. In this circuitry another microcontroller is responsible for angular velocity measurement of each motor from encoders.
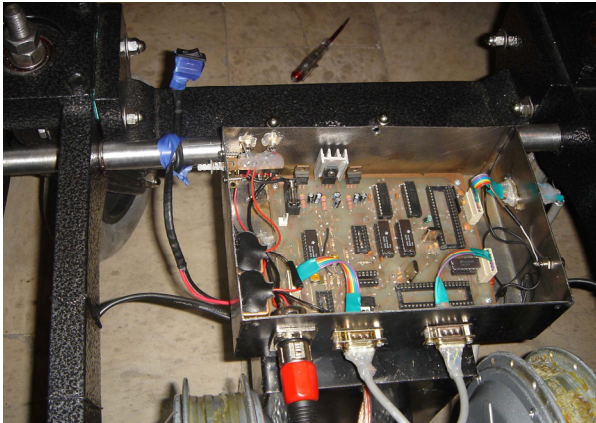

Fig. 4. The control unit of our EPW placed under the seat.

Experimental results of mere stimulation of each reference input are illustrated in Fig. 5 and Fig. 6.

VII. CONCLUSION

By combining non-holonomic mobile robots kinematics and DC motors dynamics, an accurate MIMO dynamic model has been suggested for EPW. The model was then pre-compensated by a static matrix in order to achieve further diagonal dominance and to ease system identification stage. The augmentation significantly improved the diagonal dominance of the system and provided a better way for the plant to be identified. The inputs of augmented system could be solely stimulated while both DC electric motors were operating. 100 TFM's have been estimated for the system and an uncertainty region was calculated for the system regarding weight variation and COG movement. CLM was utilized to design a controller to satisfy some criteria including safety, ride comfort and acceptable maneuverability. Robust stability was proved theoretically through a sufficient stability theorem for additive perturbations. Although the algorithm was complicated, the controller complexity was very low. Test results obtained from the microcontroller-based system showed robust stability and desired performance.
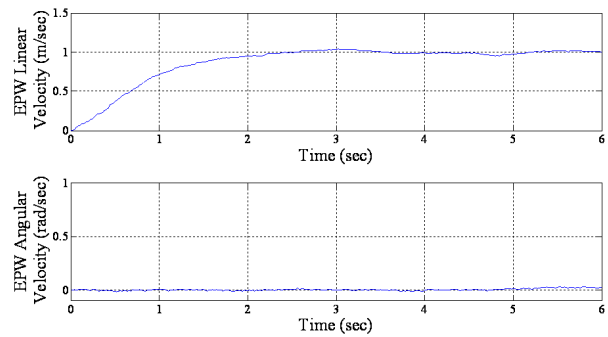

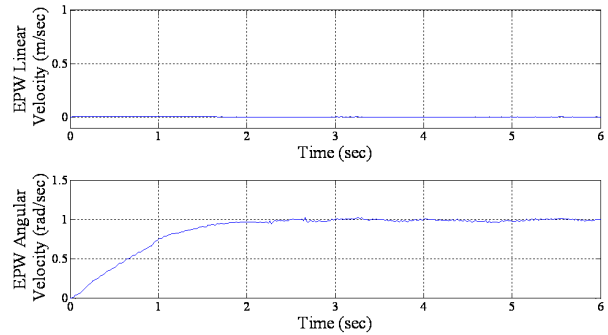Fig. 5. EPW linear and angular velocities when only the first reference input is stimulated by step command.

Fig. 6. EPW linear and angular velocities when only the second reference input is stimulated by step command.

REFERENCES

[1] M. L. Jonesand and J. A. Sanford, "People with mobility impairment in the United States today and in 2010," *Assistive Technology,* vol. 8, no. 1, pp. 43–53, 1996.

[2] B. W. Johnson and J. H. Aylor, "Design of an adaptive controller for microcomputer implementation," *IEEE Trans. Industrial Electronics,* vol. IE-33, no. 1, pp. 28–33, Feb. 1986.

[3] K. E. Brown, R. M. Inigo, and B. W. Johnson,. "Design, implementation, and testing of an adaptable optimal controller for an electric wheelchair," *IEEE Trans. Industrial Electronics*, vol. 26, no. 6, pp. 1144–1157, Nov. -Dec. 1990.

[4] C. Kauffmannl, M. Zasadzinski, and M. Darouach, "Robust optimal control design applied to an electric wheelchair," in *Proc. IEEE Int. Conf. Systems, Man and Cybernetics*, 1993, pp. 559–564.

[5] L. Boquete, R. Barea, R. Garcõa, M. Mazo, and F. Espinosa, "Identincation and control of a wheelchair using recurrent neural networks," *Engineering Applications of Artificial Intelligence*, vol. 12, pp. 443–452, 1999.

[6] L. Boquete, R. Garcia, R. Barea, and M.Mazo, "Neural control of the movements of a wheelchair," *Journal of Intelligent and Robotic Systems*, vol. 25, pp. 213–226, 1999.

[7] N. T. Nguyen, H. T. Nguyen, and S. Su, "Advanced robust tracking control of a powered wheelchair system," in *Proc. 30th Annu. Int. IEEE EMBS Conf., Vancouver*, 2008, pp. 4767-4770.

[8] K. Ogata, *Modern Control Engineering*. : 3th edition, Prentice Hall., 1996, ch.3.

[9] G. Campion, G. Bastin, and B. AndrCa-Novel, "Structural properties and classification of kinematic and dynamic models of wheeled mobile robots," *IEEE Trans. Robotics and Automation,* vol. 12, no. 1, pp. 47–62, Feb. 1996.

[10] J. M. Maciejowski, *Multivariable Feedback Design*. Cambridge: Addison-Wesley, 1989.